

PEDIATRIC ANESTHESIA MONITORING WITH THE HELP OF EEG AND ECG

L. Senhadji, G. Carrault, H. Gauvrit, E. Wodey, P. Pladys, F.
Carré

Correspondance : Laboratoire Traitement du Signal et de l'Image (LTSI), INSERM, Université de
Rennes 1, Rennes, France.
email : lotfi.senhadji@univ-rennes1.fr

PEDIATRIC ANESTHESIA MONITORING WITH THE HELP OF EEG AND ECG

L. Senhadji, G. Carrault, H. Gauvrit, E. Wodey, P. Pladys,
F. Carré

Correspondance : Laboratoire Traitement du Signal et de l'Image (LTSI), INSERM, Université de Rennes 1, Rennes, France.
email : lotfi.senhadji@univ-rennes1.fr

Abstract

This paper presents research regarding the monitoring of the brain and the adequacy of anesthesia during surgery. Particular variables are derived from EEG and ECG signals and are correlated to anesthetic gas (sevoflurane) concentration, in pediatric anesthesia. The methods used for parameter extraction are based on change detection theory and time-frequency representation. Preliminary results show that the expired anesthetic gas concentration modulates both the heart rate variability and the duration of the burst suppression. Monitors of the central nervous system and autonomic nervous system activities can be expected based on these variables.

I Introduction

During general anesthesia direct testing of the central nervous system (CNS) by means of physical examination still remains difficult. Hence, the occurrence of a CNS injury may not be detected during surgery, resulting in irreversible brain damage. Under these conditions, the monitoring of the cerebral function appears highly desirable.

The electroencephalogram is currently the most popular monitor of neurological function during general anesthesia. Various physiological perturbations, the administration of specific drugs and the depth of anesthesia may alter the structure of the EEG (Drader *et al.*, 1997). The first marker is generally a change in frequency distribution with suppression of both alpha and beta

frequency bands and the predominance of slower frequency components (Mahla, 1997). During severe cortical deterioration, burst suppression appears progressing to an isoelectric pattern (Prior, 1996). Similar patterns occur with many different classes of anesthetic agents (Mahla, 1997) and with induced hypothermia during cardiac surgery.

In the operating room, EEG might then be included in the monitoring for brain damage as well as for the assessment of the depth of anesthesia which, in clinical practice, is estimated from indirect and non specific signs including haemodynamic, respiratory, muscle and autonomic signs (Langford, 1996). Many attempts have been made to determine an accurate monitor for the adequacy and the depth of anesthesia based on variables extracted from EEG recording. The main parameters presently used are derived from the amplitude of the EEG and from its power spectrum (Bloom, 1997). Recently monitors based on the bispectrum of the EEG (Rampil, 1998) (Gajraj *et al.*, 1998) or on the quantitative analysis of middle latency auditory evoked potentials (MLAEP) have been introduced (Huowg *et al.*, 1999). The techniques based on temporal and spectral representation appear insufficient, those based on MLAEP and bispectrum analysis need further validation (Todd, 1998) (Gajraj *et al.*, 1998) (Hall and Lockwood, 1998). None of these monitors provide information of high specificity and they have to be interpreted in relation to the context and the nature of the surgical operation.

The ECG signal is routinely monitored during general anesthesia. Normal sinus rhythm results from the influence of cardiac autonomic nervous system on the electrophysiology of the sino-atrial node. Beat to beat variability of the heart rate (HR) is caused by a fluctuating balance of sympathetic to parasympathetic tone and reflects the influence of autonomic nervous system on cardiac functioning.

Power spectrum analysis has been shown to be of significance in the evaluation of HR variability and in providing an estimation of sympathetic/parasympathetic balance (Akselrod *et al.*, 1981) (Malliani *et al.*, 1991). The high frequency (HF) spectral components correspond to parasympathetic vagal activity mediated by the respiratory center (respiratory arrhythmia). The lower frequency (mid frequencies = MF and low frequencies = LF) are influenced by both sympathetic and parasympathetic activity. General anesthesia has been shown to depress HR variability (Ireland *et al.*, 1996 ; Galletly *et al.*, 1998 ; Kato *et al.*, 1992 ; Kawamoto *et al.*, 1994 ; Mazerolles *et al.*, 1996) and to inhibit HR response to changes in blood pressure (Schubert *et al.*, 1997). Moreover a dose related decrease in the cardiac autonomic nervous system activity in both vagal and sympathetic nerves activity has been found after isoflurane. Donchin *et al.*, (1985) have shown that the amplitude of respiratory sinus arrhythmia decreases in the course of isoflurane-nitrous oxide anesthesia and that all the components of power spectral analysis of the HR variability increase in the recovery period. The effect of general anesthesia with inhalation anesthetic has been further investigated by Galletly (*et al.*, 1998) who found that total power and powers in the three frequency bands decreased under general anesthesia and that the depression was significantly greater in MF components without any difference between halothane and isoflurane. These results are confirmed by Deutschman *et al.*, (1994) who have found that in adult patients, propofol, an IV anesthetic, reduces high frequency variability to a lesser degree than low frequency variability and that the power spectral profile evolves with the level of anesthesia. Such significant variations of HR power spectrum parameters were also reported by Schubert (*et al.*, 1997) during general anesthesia for abdominal surgery with a combination of thiopental sodium, fentanyl, isoflurane or enflurane and nitrous oxide and after pentobarbital in dogs (Kawamoto *et al.*, 1994).

The final aim of this work is to monitor the brain activity and the adequacy of the anesthesia during surgery. To do so, both EEG and ECG signals, recorded in children, in the operating room have been studied. The EEG analysis focuses on the spatio-temporal distribution and evolution of

burst suppression patterns, their characterization (in time domain, frequency domain and time-frequency domain), in relation to their origin (pharmacological, physiological, pathological), and their correlation with the RR intervals, derived from the ECG. Other studies for CNS monitoring using the EEG, both in operating room and intensive care units, are being conducted in the framework of the European Project IBIS (Ibis, 1997).

A preliminary database, presented in the next section, was recorded and analyzed during minor surgical operations in which a single rather than a combination of anesthetic agents was appropriate clinically and where the risk of cerebral injuries was very low. Therefore the changes in the ECG and EEG signals will only be correlated to the concentration of the anesthetic gas used here (sevoflurane). As mentioned in the previous paragraph, abrupt modifications appear in the EEG and ECG signals during general anesthesia. The determination of the time of their occurrence is the first step toward a quantitative study of anesthesia. This is the objective of section III where two specific algorithms, based upon rupture detection theory (Basseville and Nikiforov, 1993), are described. Results of segmentation are discussed in section IV and promising perspectives are mentioned.

II Data base

Ten ASA physical status I or II¹ children (2-5 years old) who required elective surgery were studied after the protocol had been approved by the Human Studies Committee and informed parental consent had been obtained. All children were premedicated 30 min. before induction of anesthesia with 0.3 mg/kg rectal midazolam and were NPO (*nil per os*) for 4 hr. preoperatively. An inhaled induction of anesthesia was started with sevoflurane (8%) in oxygen, without nitrous oxide, through an open circuit without soda lime absorber. Children were breathing spontaneously during

¹ Classification of patient status provided by the American Society of Anesthesiologists. I : A normal healthy patient, II : A patient with mild systemic disease.

induction until endotracheal intubation. After placement of an intravenous line, the trachea was intubated and the lungs were ventilated, to maintain normocarbida at the same frequency (30 cycles/min) for all children. Inspired concentration of sevoflurane was maintained, at 8% until a steady state was obtained, then inspired concentration of the anesthetics gas was decreased every minute about 1%. When clinical depth of anesthesia appeared inadequate, decrease in sevoflurane concentration was stopped and a rapid increase was performed in order to obtain an appropriate depth of anesthesia for starting the surgical procedure. Anesthetic gas concentration and carbon dioxide concentration were measured from gas samples continuously aspirated from an elbow connector added to the endotracheal tube. ECG, EEG, capnograms as well as inspired and expired gas concentrations (sevoflurane) were recorded simultaneously and continuously. The EEG signals were recorded by means of bi-frontal electrodes.

Since pediatric anesthesia has not attracted particular attention during recent years, a unique indicator of consciousness from HR signals is not clearly established. Evidence for early expression of possible awareness was experimentally retrieved from the HR signal. Figure 1 shows a typical sequence of the expired gas concentration, the RR interval, its rapid fluctuation (spontaneous heart rate variability SHR_V) and its slow trend (absolute values of heart Rate AVHR). Just before the awareness (anesthetic concentration is close to zero), we observed a decrease in the HR frequency and a progressive variability in rate. At the onset of awareness, HR frequency increases abruptly and the variability becomes more important. This typical evolution was observed on 9 of the ten patients, the 10th having slightly different behavior (Figure 2).

Figure 1

Figure 2

In patient 10, HR variability is always present suggesting that the autonomic nervous system is not completely depressed even though the patient has been correctly anesthetized. Despite this last remark, It could be noticed that just before and after the onset of awareness a similar global behavior is observed (decrease in cardiac frequency, the evidence of variability and rapid increase in cardiac frequency).

The behavior of the EEG signal (left channel) for patient n°1 and patient n°10 are reported respectively in Figure 3 and Figure 4.

Figure 3

Figure 4

Even for comparable gas concentration, the characteristics / components of the EEG varied from one patient to another. Figure 3, shows the EEG dynamics for the patient n°10 where a "spike-like" activity appeared and a long-term stationary signal is only observed at an expired sevoflurane concentration around 3%. For patient n°1, the anesthetic agent induced only a burst suppression activity. As for patient 10, a long-term stationary signal is recovered for an expired gas concentration close to 4% (Figure 4).

III Change detection in a signal

From a formal point of view, this problem belongs to the so-called rupture detection which consists of confronting the two following composite hypotheses:

$$\begin{aligned}
 H_o & : x_o \dots x_n \text{ follow the model } \theta_o \\
 H_1 & : x_o \dots x_{r-1} \text{ follow the model } \theta'_o \quad (1) \\
 & \quad x_r \dots x_n \text{ follow the model } \theta_1
 \end{aligned}$$

where θ is a family of models. From a practical point of view, we have to choose between the two previous hypotheses H_o and H_1 , to localize the time instant of change r and, if necessary, to estimate the models θ_o , θ'_o and θ_1 before and after the rupture. Since the models θ_o , θ'_o and θ_1 are generally unknown, the choice between the two hypotheses is done using the generalized likelihood ratio.

III.1 Detection of bursts and suppressions in the EEG signal

A typical situation observed during an anesthesia is reported in Figure 5. The goal is to detect the abrupt changes occurring within the signal that alternate between silent periods (the suppressions) and important neuronal discharges (the bursts).

Figure 5

The examination of this previous situation suggests testing the two following hypotheses:

$$\begin{aligned}
 H_o & : x_o, \dots, x_n \text{ follow the law } P_0(x_o, \dots, x_n) \\
 H_1 & : x_o, \dots, x_{r-1} \text{ follow the law } P_0(x_o, \dots, x_{r-1}) \\
 & \quad x_r, \dots, x_n \text{ follow the law } P_1(x_r, \dots, x_n)
 \end{aligned}$$

The problem is then equivalent to detecting an abrupt change, occurring at the time instant r , in the variance of the samples x_0, \dots, x_n . If the samples x_0, \dots, x_n are mutually independent under H_0 and H_1 and if the observation vector $X=[x_0, \dots, x_n]$ follows a centered gaussian law, it is simple to show that the instantaneous likelihood ratio can be written as:

$$L_n = \frac{P_1(x_n)}{P_0(x_n)} = \ln \frac{\hat{\sigma}_0}{\hat{\sigma}_1} + \left(\frac{1}{\hat{\sigma}_0^2} - \frac{1}{\hat{\sigma}_1^2} \right) \frac{x_n^2}{2}$$

which, before the change (under H_0 hypothesis), has the following mean value:

$$E_0(L_n) = \ln \frac{\hat{\sigma}_0}{\hat{\sigma}_1} + \frac{1}{2} \left(1 - \frac{\hat{\sigma}_0^2}{\hat{\sigma}_1^2} \right)$$

while, after the change (under H_1 hypothesis), the mean value of L_n becomes :

$$E_1(L_n) = \ln \frac{\hat{\sigma}_0}{\hat{\sigma}_1} + \frac{1}{2} \left(\frac{\hat{\sigma}_1^2}{\hat{\sigma}_0^2} - 1 \right)$$

In such a case, we can estimate the time instant r by using the so-called Page-Hinkley algorithm or the cumulative sum applied to the likelihood ratio L_n . This last algorithm presents moreover some interesting theoretical properties such as the control of the mean time between false alarm in function of the decision threshold λ . It is sometimes preferable to compute the quantity:

$$\tilde{L}_n = \frac{P_1(x_n)}{P_0(x_n)} - E_0 \left\{ \frac{P_1(x_n)}{P_0(x_n)} \right\} = \left(\frac{1}{\hat{\sigma}_0^2} - \frac{1}{\hat{\sigma}_1^2} \right) \frac{x_n^2}{2} - \frac{1}{2} \left(1 - \frac{\hat{\sigma}_0^2}{\hat{\sigma}_1^2} \right)$$

to guarantee that, before the change, the mean value $E_0(\tilde{L}_n) = 0$ and after the change, it is :

$$E_1(\tilde{L}_n) = \frac{1}{2} \left(\frac{\hat{\sigma}_1^2}{\hat{\sigma}_0^2} - \frac{\hat{\sigma}_0^2}{\hat{\sigma}_1^2} \right) - 1$$

In practice, nothing warrants the samples are mutually independent. We can, in such situation, prewhiten the EEG observation by means of an autoregressive (AR) filter estimated on line. The previous algorithm could then be applied on the innovation e_n of the AR model which fulfil the required proprieties. Finally, this algorithm requires the knowledge of the variances σ_o^2 and σ_l^2 (θ_o and θ_l respectively in the general case). These quantities can be computed from a maximum likelihood estimation and are calculated on two distinct windows: the first one, large and growing for σ_o^2 (θ_o resp.), the second one, short and sliding for σ_l^2 (θ_l resp.). The whole algorithm is summarized in the following picture:

Figure 6

IV Rupture detection in RR interval

The examination of the RR interval during anesthesia clearly shows (Figure 1 and Figure 2) two types of events: *i*) a slope change within the slow trend AVHR of the RR interval and *ii*) a spectral rupture into the rapid trend SVHR of the RR interval. This last remark explains why HR signal is low pass filtered (a comb filter) to build the AVHR trend, while the SHR V is deduced from:

$$\begin{aligned} SHR V (i) &= HR (i) - AVHR (i) \quad \text{where} \\ AVHR (i) &= \frac{1}{M} \sum_{j=0}^{M-1} HR (i - j) \end{aligned} \quad (1)$$

Since abrupt changes in the AVHR and SHRV may provide an indicator of awareness in depth anesthesia, rupture detection algorithms as described in the last section, can be considered for their estimation. The whole processing scheme is depicted Figure 7. Data are first filtered in order to eliminate low frequency drift and high frequency components, merged with the signal, due mainly to the patient's movements in the initial and final phases of the anaesthesia. The ECG signal is then processed by the length transformation proposed by Gritzali (1988) and an optimal threshold is computed to detect the QRS occurrence in order to construct the HR variability sequence.

Figure 7

IV.1 Change within AVHR

The analysis of the AVHR trend suggests the modeling of the observations as a linear slope embedded in a centered white Gaussian noise, with variance σ^2 (figure 1 and figure 2). In this context, the set of parameter θ is then (a, b, σ^2) and (1) becomes:

$$\begin{aligned} H_o : y(k) &= a_o (k - 1) + b_o + e_o(k) \quad \text{for } 1 \leq k \leq N \\ H_1 : y(k) &= a_o (k - 1) + b_o + e_o(k) \quad \text{for } 1 \leq k \leq r - 1 \\ & y(k) = a_1 (k - 1) + b_1 + e_1(k) \quad \text{for } r \leq k \leq N \end{aligned}$$

In this context and after straightforward calculation, L_k corrected by its mean under H_o is equivalent to :

$$w(k) = \frac{\sigma_o^2}{2\sigma_1^2} \left[\left(\frac{\sigma_1^2}{\sigma_o^2} - 1 \right) + 2 \frac{e_o(k)e_1(k)}{\sigma_o^2} - \left(\frac{\sigma_1^2}{\sigma_o^2} + 1 \right) \frac{e_o^2(k)}{\sigma_o^2} \right]$$

where $e_i(k)$ (for $i=0, 1$) is the innovation of model θ_i . (a, b, σ^2) are estimated by maximizing the likelihood, let :

$$\hat{a}_i = \frac{\sum_{k=1}^L ky(k) - \frac{1}{L} \sum_{k=1}^L k \left(\sum_{k=1}^L y(k) \right)}{\sum_{k=1}^L k^2 - \frac{1}{L} \left(\sum_{k=1}^L k \right)^2}$$

$$\hat{b}_i = \frac{1}{L} \sum_{j=1}^L (y(k) - k\hat{a}_i)$$

$$\hat{\sigma}_i^2 = \frac{1}{L} \sum_{j=1}^L (y(k) - k\hat{a}_i - \hat{b}_i)^2$$

$\hat{a}_0, \hat{b}_0, \hat{\sigma}_0^2$ are estimated recursively on a large and growing window while $\hat{a}_1, \hat{b}_1, \hat{\sigma}_1^2$ are computed on a short sliding window as described above. The cusum test is then used to compute the following quantities:

$$S(k) = S(k-1) + w(k) + \delta$$

$$m(k) = \max_{1 \leq j \leq k} (S(j))$$

$$t_{\min} = \arg \max_{1 \leq j \leq k} (S(j))$$

a change is decided if $S(k)-m(k) > \lambda$ and the rupture time r is estimated by $r = t_{\min}$. The threshold λ is selected in order to guarantee a certain mean time between false alarm while δ is a positive drift corresponding to the minimum jump to detect.

V Preliminary results

In this section preliminary results obtained on EEG burst suppression detection using the method described above and the analysis of the SVHR variability are reported. The detection of the changes in the AVHR has been reported in (Gauvrit *et al.*, 1998) and will not be illustrated here.

Figure 8a depicts an example of the segmentation procedure applied to the EEG signal. The burst suppression patterns continue and are well detected in the first minute or so after the expired sevoflurane concentration starts to decrease (Figure 8c), the burst duration increasing while the suppression duration decreases (Figure 8b). Similar behavior has been observed in the other patients but at different individual expired anesthetic concentration levels. Burst activity appears for expired gas concentration between 3.5% and 5.5% for patient n°10, while for patient n°1 such activity occurs between 3% and 4.5%.

Figure 8

The study of the SVHR curves has been conducted by means of a time-frequency analysis. Figure 9 shows the time-frequency evolution of the SVHR component when the anesthetic agent concentration decreases. We observe in the first part of the time frequency plan (before time 400s) a unique frequency component at 0.5 Hz. It is induced by the artificial respirator and not by the autonomic nervous system which is strongly depressed. When anesthetic agent concentration decreases (after 400s), the autonomic activities appear and sympathetic and parasympathetic influences are highlighted by the time frequency representation. Figure 10 is the analogue of the Figure 9 but for patient n°10. With the artificial respirator contribution, low frequency components are observed underlining the fact that the autonomic nervous system is not total depressed. After 300 s and as in the previous example, effects of sympathetic and parasympathetic tonus can be retrieved from the time frequency plan.

Figure 9

Figure 10

These two examples point out the difficulty of assessing adequacy and depth of anesthesia when they are evaluated based on indirect indicators or minimum alveolar concentration (MAC). An indicator based on the rate of depression of the autonomic nervous system could be used to evaluate the adequacy of anesthesia. Rupture detection framework, as previously described, can then be applied to detect a change in the SVHR signal using a time frequency representation, rather than the raw data; studies are presently being conducted in this direction.

VI Conclusion

One focus of this work was to show how rupture detection could be adapted to the monitoring of anesthesia. This approach has already shown its value in the biomedical field for SEEG segmentation in epilepsy (Wendling *et al.*, 1997) and for multi-hypothesis classification in EMG (Khalil and Duchêne, 1999).

Two different strategies can be adopted. The first one, which has been reported here, consists of transforming the original data into a new sequence such that, if a change occurs, it appears clearly on the new sequence by a jump into its mean value. The second one consists of transforming the signal and applying the previous framework on the new domain.

Our research is still in progress, so only preliminary results are shown here. However, its feasibility was investigated in several patients and satisfactory results were shown. Further developments are directed towards increasing the information that could be extracted from our protocol analysis. It is motivated by the fact that the ECG and the EEG signals are not fully exploited for assessing the depth and adequacy of anesthesia especially in the pediatric context. It is also motivated by the following :

1. Anaesthetic concentrations are currently used by clinicians as an indicator of depth of anesthesia. Standard concentration values such as MAC (minimum alveolar concentration) are established as a function of the patient's age. They give a pseudo gold standard to measure the powerfulness of each anaesthetic gas. They also give a reference value to quantify the depth of anesthesia. However, they are not specific or necessarily equally appropriate in every patient.
2. Regulation of the heart rate by autonomic nervous system is now well established. Pharmacological effects of volatile anesthetics agent on the ANS and its regulation would allow a better understanding of the relationships between gas, ANS and the effects on the central nervous system during pharmacological sleep.
3. If robust markers and robust relationships (reproducible for a given population), between gas concentration (GC) and the depth of anaesthesia (DA), could be defined from heart rate variability or EEG analysis, the influence of others drugs, such as morphine used for analgesia, would be better identified and their usefulness, particularly during classical anesthesia, might then be quantifiable taking into account the previous relation GC-DA, pain and drug.

VII References

Akselrod, S., D. Gordon, F. Ubel, D. Shannon, A. Berger and R. Cohen (1981). Power spectrum analysis of heart rate fluctuation: a quantitative probe of beat to beat cardiovascular control. *Science* 213:220.

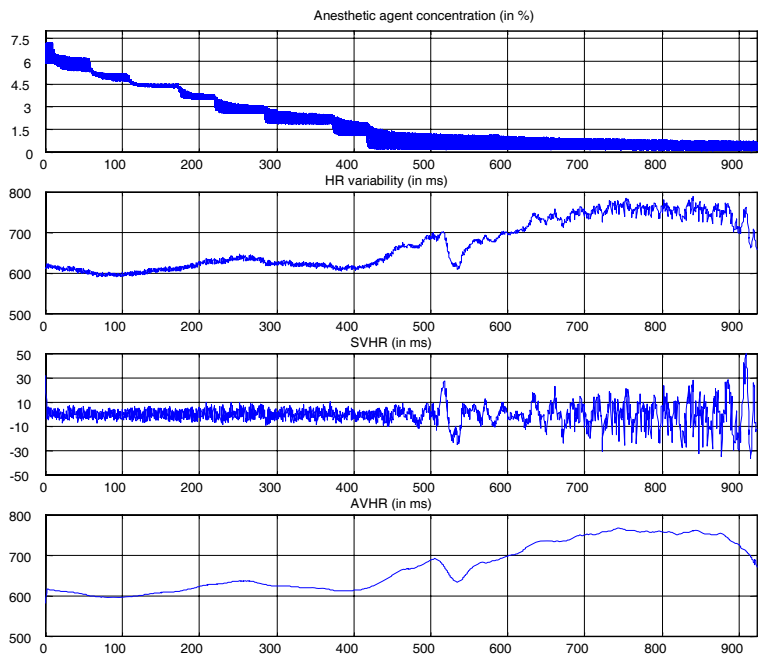
Basseville, M. and I. Nikiforov (1993). *Detection of abrupt changes, Theory and application*. Prentice-Halle, Englewood Cliffs, NJ.

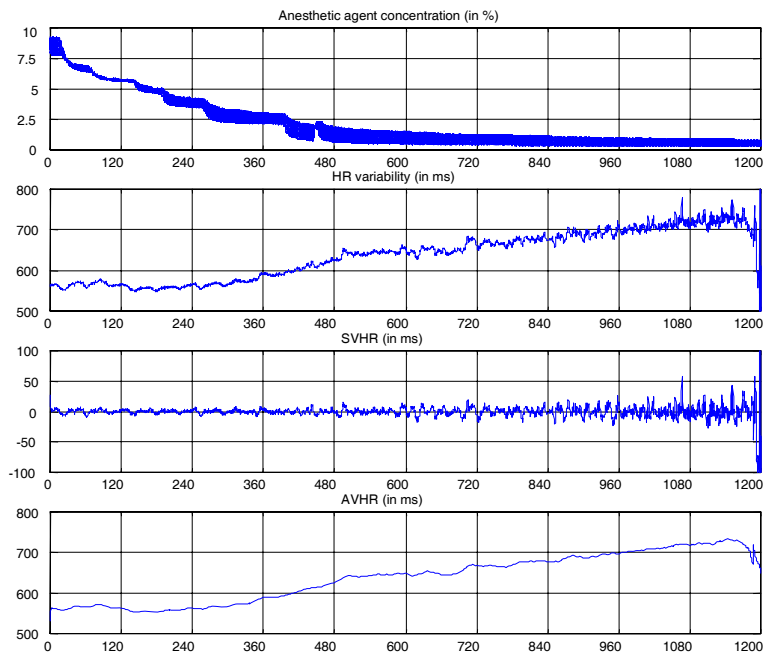
- Bloom, M.J. (1997). EEG monitoring: intraoperative application. *Anesthesiology clinics of North America*. 15: 551-571.
- Deutschman, C.S., A.P. Harris and L.A. Fleisher (1994). Changes in heart rate variability under propofol anesthesia: a possible explanation for propofol induced bradycardia. *Anesthesia Analgesia*. 79 : 373-377.
- Donchin, Y., J.M. Feld and S.W. Porges (1985). Respiratory sinus arrhythmia during recovery from isoflurane-nitrous oxide anesthesia. *Anesthesia Analgesia*. 64: 811-815.
- Drader, K.S. and I.A. Herrick (1997). Carotid endarterectomy: monitoring and its effect on outcome. *Anesthesiology clinics of North America* 15: 613-628.
- Gajraj, R.J., M. Doi, H. Mantzonidis and G.N.C. Kenny (1998). Analysis of the EEG bispectrum, auditory evoked potentials and the EEG power spectrum during repeated transitions from consciousness to unconsciousness. *British Journal of Anesthesia* 80: 46-52.
- Galletly, D.C., A.M. Westenberg, B.J. Robinson and T. Corfiatis (1998). Effect of halothane, isoflurane and fentanyl on spectral components of heart rate variability. *British Journal of Anaesthesia* 80: 72:77.
- Gauvrit, H., G. Carrault, P. Pladys, E. Wodey and F. Carré (1998). Monitoring of heart rate during paediatric anesthesia, *Proc. CIC*, 1998.
- Gritzali, F. (1988). Towards a generalized scheme for QRS detection in ECG waveforms. *Signal Processing* 15: 183-192.
- Hall, J.D. and G.G. Lockwood (1998). Bispectral index: comparison of two montages. *British Journal of Anesthesia* 80: 342-344.
- Huowg, J.W. , Ying-Ying Lu, A. Nayak and R.J. Roy (1999). Depth of anesthesia estimation and control *IEEE-Transaction in Biomedical Engineering* 46: 71-81.
- IBIS (1997), Improved Monitoring for Brain Dysfunction in Intensive Care and Surgery. EC contract n° BMH4-97-2570, 1997.

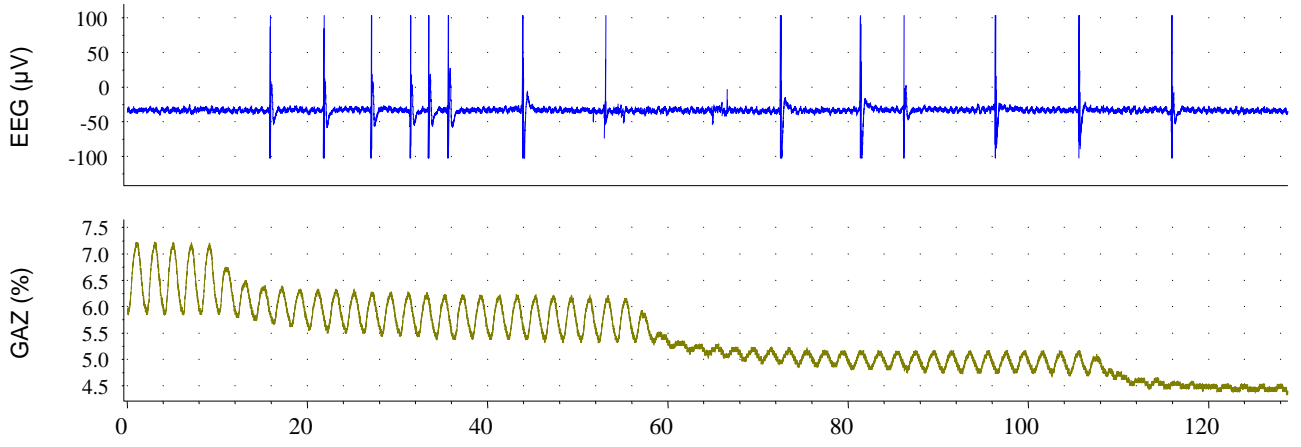
- Ireland, N., J. Meagher, J.W. Sleight and J.D. Henderson (1996). Heart rate variability in patients recovering from general anaesthesia. *British Journal of Anaesthesia* 76: 57-62.
- Kato, M., T. Komatsu, T. Kimura, F. Sugiyama, K. Nakashima and Y. Shimada (1992). Spectral analysis of heart rate variability during isoflurane anesthesia. *Anesthesiology* 77: 669-674.
- Kawamoto, M., K. Kaneko, K. Hardian and O. Yuge (1994). Heart rate variability during artificial ventilation and apnea in brain damaged rabbits. *Am J Physiol* 6: 271; H410.
- Khalil, M and J. Duchêne (1999) Detection and classification of multiple events in piecewise stationary signals: comparison between autoregressive and multiscale approaches. *Signal Processing* 75: 239-252.
- Langford, R.M. (1996). Clinical applications of cerebral monitoring. *Computer methods and programs in biomedicine*. 51: 29-33.
- M.E. Mahla, M.E. (1997). The electroencephalogram in operating room. *Seminar in anesthesia*, 16: pp. 3-13.
- Malliani, A., M. Pagani, F. Lombardi and S. Cerutti (1991). Cardiovascular neural regulation explored in the frequency domain. *Circulation* 84: 482-92.
- Mazerolles, M., J.M. Senard, P. Verwaerde, M.A. Tran, J.L. Montastruc, C. Virenque and P. Montastruc (1996). Effects of pentobarbital and etomidate on plasma catecholamine levels and spectral analysis of blood pressure and heart rate in dogs. *Fundam Clin Pharmacology* 10: 298-303.
- P.F. Prior, P.F. (1996). The rational and utility of neurological investigations in clinical monitoring for brain and spinal cord ischaemia during surgery and intensive care. *Computer methods and programs in biomedicine*. 51:13-27.
- Rampil, I.J. (1998). A primer for EEG signal processing in anesthesia. *Anesthesiology*. 89: 980-1002.
- Schubert A., J.A. Palazzolo, J.M. Brum, M.P. Ribeiro and M. Tan (1997). Heart rate, heart rate variability, and blood pressure during perioperative stressor events in abdominal surgery. *J Clin Anesth*. 9: 52-60.

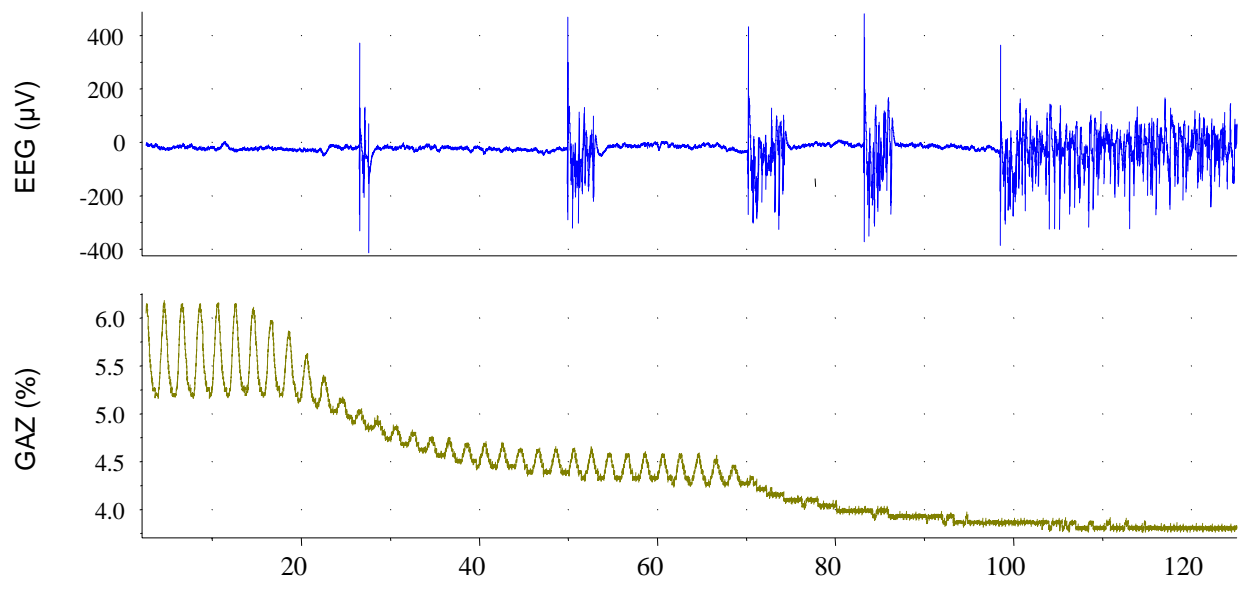
Todd, M.M, (1998). EEGs, EEG processing and the bispectral index. *Anesthesiology*. 89: 815-817.

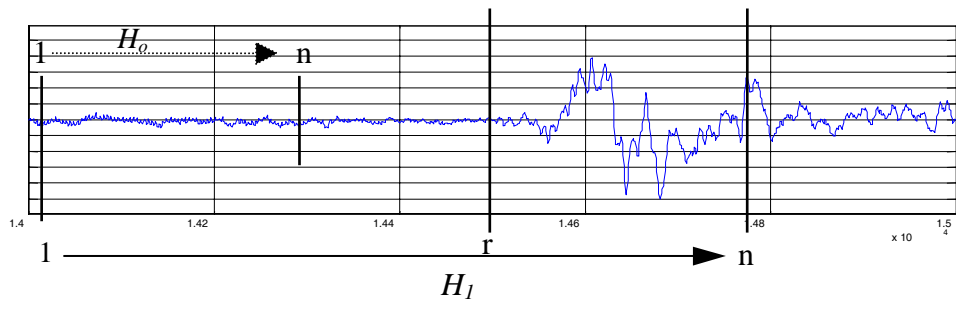
Wendling, F., G. Carrault and J.M. Badier (1997). Segmentation of Depth-EEG Seizure Signals : Method Based on a Physiological Parameter and Comparative Study. *Annals of Biomedical Engineering* 25: 1026-1039.

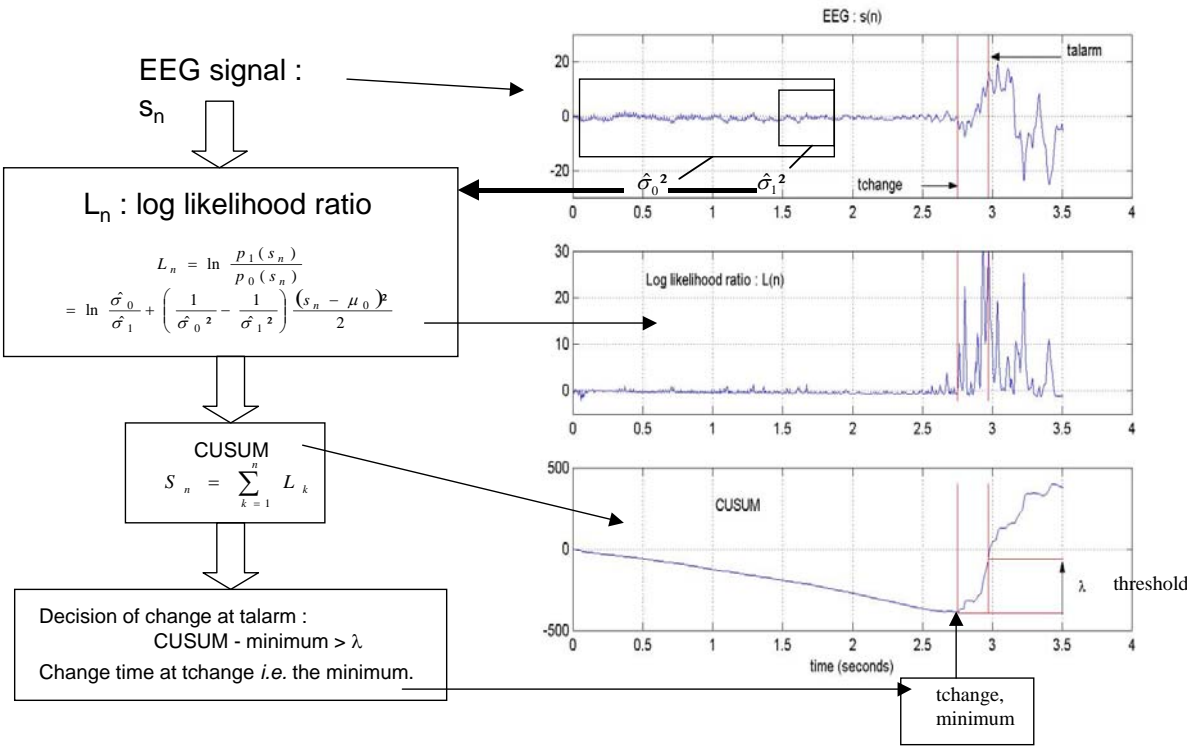


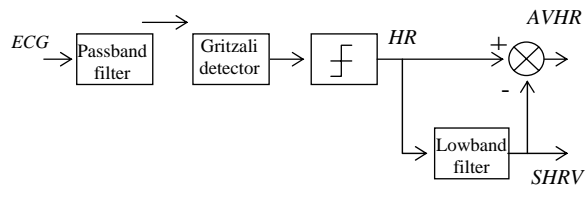


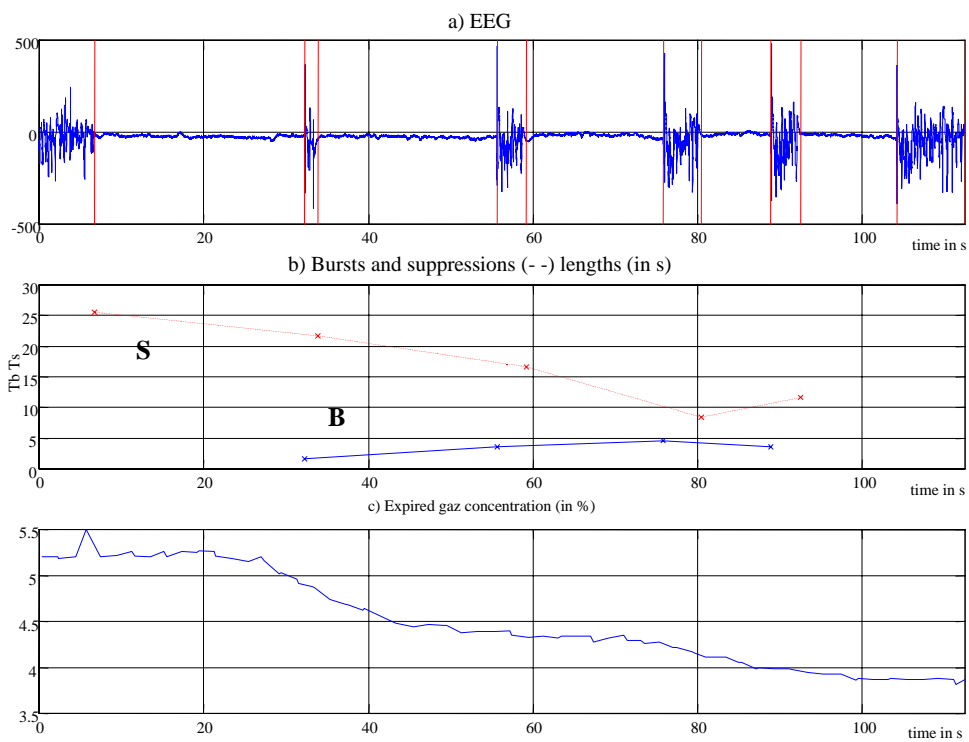


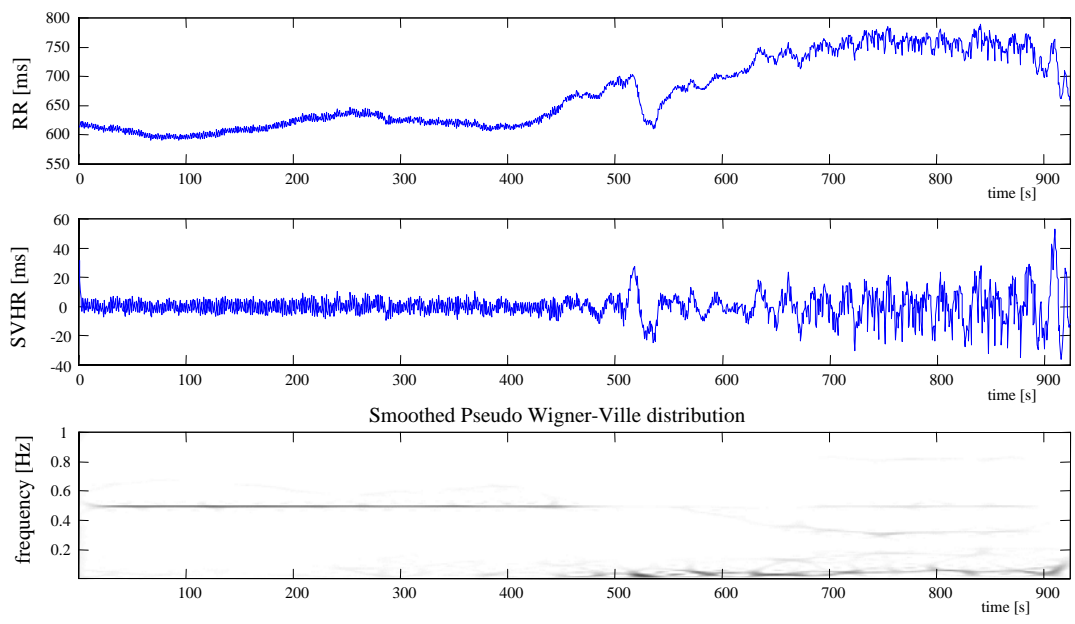


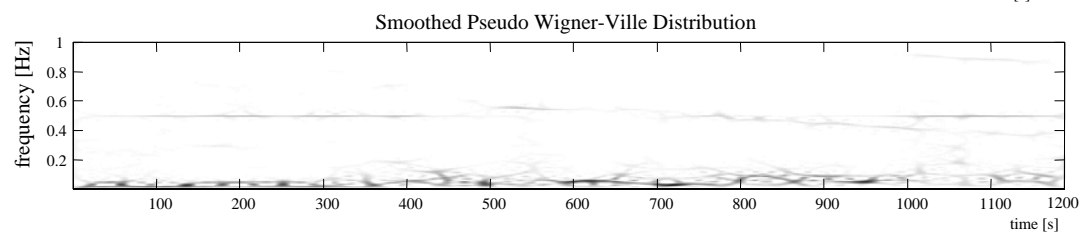
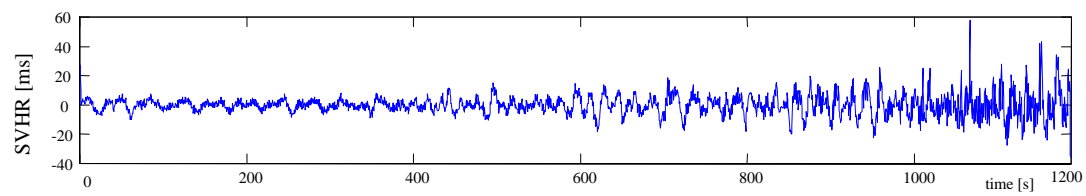
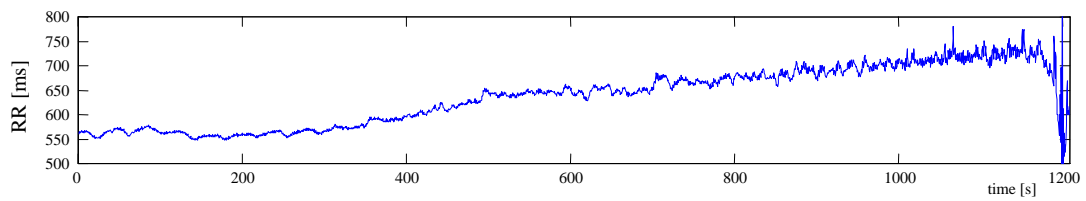












Legends

Figure 1: Behavior of the HR and anesthetic agent concentration up to awareness (patient n°1).

Figure 2: Behavior of the HR and anesthetic agent concentration up to awareness (patient n°10).

Figure 3: EEG behavior and anesthetic gas concentration for patient n°10 (time in sec).

Figure 4: EEG behavior and anesthetic gas concentration for patient n°1.(time in sec).

Figure 5: EEG signal showing burst suppression patterns.

Figure 6: Description of the Burst Suppression Algorithm.

Figure 7: Extaction of the HR variability curves.

Figure 8: Burst Suppression activity for the patient n°1.

Figure 9:SVHR variability, up to awareness, of the patient n° 1.

Figure 10: SVHR variability, up to awareness, for the patient n°10